JOURNAL OF MATERIALS SCIENCE 27 (1992) 3424–3434

Water absorption, swelling, rupture and salt release in salt–silicone rubber compounds

R. SCHIRRER, P. THEPIN
ICS(CRM-EAHP), 4 rue Boussingault, F-67000 Strasbourg, France
G. TORRES
Rhône Poulenc, P.O. Box 62, F-69192 Saint-Fons, France

Water vapour diffuses rapidly in silicone polydimethylsiloxane (PDMS) rubber. In a PDMS–salt compound surrounded by water, the water which has entered the rubber is absorbed by the salt particles, creating an osmotic pressure in the rubber. This pressure leads to internal cracks in the rubber, which eventually percolate and result in a salt exchange between the rubber–salt compound and the surrounding pure water. The absorption and rupture phenomena were derived, measured, and quantitatively analysed. Equations describing the onset and propagation of the microcracks in the silicone were derived as a function of rubber fracture toughness, tensile modulus and osmotic pressure of the salt. A single figure summarizes three possible situations: (1) the salt plus water pockets in the compound reach an equilibrium without cracking, (2) the salt pockets are fully dissolved, and cracking occurs, (3) the salt pockets generate microcracks before full dissolution of the salt. Finally, the salt release has been quantitatively related to the PDMS tensile modulus, fracture surface energy, and salt grain size.

Nomenclature

$\mathring{a}$	crack speed
$\langle A \rangle$	mean distance between two salt grain centres
$\langle B \rangle$	mean distance between two salt grain borders
$\langle D \rangle$	mean cavity diameter in rubber ($D = 2r$)
$\langle D_0 \rangle$	mean diameter of salt grains or mean initial cavity diameter ($D_0 = 2r_0$)
E	tensile modulus
G	shear modulus
G_1	fracture toughness
G_{1c}	critical value of G_1 at rupture instability
h_0	sample height (fracture experiment)
k	reduced fracture coefficient for holes in rubber
K_1	fracture toughness (MPa $m^{1/2}$)
K_{1c}	critical fracture toughness at rupture instability
M	sample mass
M_0	initial value of M
n	moles of particles formed upon solution of 1 mol solute ($n = 2$ for NaI)
P	pressure in a cavity in the rubber
P_c	critical value of P at rupture instability
Q	salt volume in a rubber–salt compound
Q_0	initial value of Q
R	0.082 055 dm^3 10^5 Pa K^{-1} mol^{-1}
r	radius of a spherical cavity in the rubber
r_0	initial value of r
S	sample surface
S_0	initial value of S
S_2	volume fraction of solute in solution
T	temperature
t	time (s)
V	volume of the swollen rubber–salt sample
V_0	initial volume of the rubber–salt sample
$\langle v_c \rangle$	mean microcrack front speed
W	energy per unit volume in a rubber sample under stress
α	experimental best fit coefficient
β	experimental best fit coefficient
Δh	displacement
φ	salt volume fraction in the compound
Φ	water flow in PDMS per unit time and unit area at the PDMS–salt interface
λ	extension ratio of a spherical cavity in the rubber
λ_c	critical value of λ at rupture instability
v_2	molar volume
π	osmotic pressure
τ_c	critical duration for swelling a salt pocket up to rupture

1. Introduction

The diffusion and absorption of liquid, especially water, in rubbers is of major practical importance. This absorption leads to drastic decreases of the mechanical or electrical properties of the rubber. As rubber often contains solid inclusions, the amount of absorbed water is much greater than the value expected for pure rubber. If the inclusions are water soluble, the

0957–4530

water is absorbed by means of osmosis through the surrounding polymer, which acts like a semi-permeable membrane. The general problem of water absorption, swelling of the solid inclusions and the equilibrium water content, has been largely studied in the literature. Flory gave an estimation of the equilibrium solubility of water in pure polymers [1]. Other authors studied the case of several polymers containing soluble inclusions from different points of view, particularly the equilibrium between the osmotic pressure and the water content of the material [2–7]. In fact, cracks have even been recorded in silicone rubbers containing $CoCl_2$ [8]. Water permeation, sorption equilibrium and kinetics in silicone rubbers containing sodium chloride salt have been extensively investigated in early work by Barrie and Machin [9, 10]. As the rubber is often a semi-permeable membrane for salt water, none of the cited literature deals with the salt exchange between the rubber–salt compound and the surrounding water. Recent literature on the specific problem of salt release by means of a rubber–salt compound has been published [11–19]. These authors experimentally examined the flow rate of various active molecules embedded in silicone rubbers as a function of several experimental parameters, such as molecular activity, concentration, grain size and temperature. They clearly stated the general mechanisms of the flow, particularly the microcracking of the rubber, but no attempt has been made to quantify these results relating osmotic pressures of salts to rupture properties of rubbers.

2. Overall mechanism: phenomenology

The main feature of the rubber–salt compound immersed in water is that the salt flow from the compound towards the surrounding water is time independent up to at least 80% release of the salt content. Therefore, the flow mechanism is not a diffusion mechanism. Moreover, it is known that rubbers such as poly-dimethylsiloxane (PDMS) are not permeable to dissolved salts, and that the salt diffusion coefficient in PDMS is several orders of magnitude lower than that necessary to explain the observed salt flows. Therefore, the mechanism controlling the salt flow as observed in this work is briefly described below [11–19].

2.1. General mechanism

The preparation of PDMS–salt compounds has been described in the literature. The salt is kept dry during the preparation, and homogeneously dispersed in the compound. The compound is immersed in a large volume of water. The salt content of the water is regularly measured, and exhibits an almost linear increase, up to 80–90% total salt release of the compound. The following mechanisms have emerged from a review of the literature (Fig. 1).

(a) PDMS is a semi-permeable membrane for salt, and diffusion cannot account for the observed release.

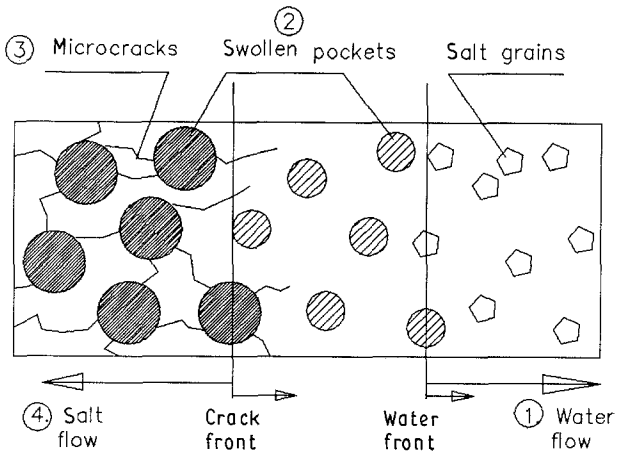

Figure 1 The four steps of water diffusion, rubber swelling, rupture and salt flow towards the surrounding water as described in [11–19].

(b) Water vapour diffusion through PDMS is very rapid, although the water content in PDMS is very low. Liquid water cannot diffuse through PDMS.

(c) The water entering PDMS is trapped by the salt grains, that finally form large pockets in which the salt is fully dissolved (for highly soluble salts).

(d) The osmotic pressure created in a pocket may be large enough to create microcracks around the pockets.

(e) The microcracks grow and finally percolate, creating small pipes between the salt pockets and the surrounding water.

(f) The osmotic differential pressure between the pockets and the external water creates a salt flow from the pocket towards the water through the micro-pipes.

(g) The salt flow is constant, unlike a diffusion flow, due to the constant crack growth speed.

2.2. Experimental simulation

One of the major uncertainties in the mechanism lies in the ability of PDMS rubber to exhibit microcracks under hydrostatic pressure. Some authors [8] have already reported such behaviour, but a direct visualization of the initiation of the micro-cracks and kinetics was necessary. As the cracks are filled with salt water as soon as they initiate, they cannot be easily visualized under the microscope. Therefore, an experiment with gas has been performed in the following way.

A pure PDMS cylinder (about 1 cm diameter, 2 cm long) was prepared with a few small internal bubbles (0.1–1 mm diameter). The sample was introduced into a high-pressure transparent chamber, in which the air was pressurized to 3 MPa. A video camera recorded the image of the sample. The internal bubbles first shrunk, and after 1 h, due to the gas permeability of the PDMS, they reached the equilibrium external pressure and expanded to their original size. The external pressure was suddenly dropped to atmospheric pressure. The internal bubbles were then subjected to a hydrostatic negative pressure of 3 MPa. A few seconds later, they blew up and microcracks initiated very rapidly around them. The sample was fully microcracked within 10 min (Fig. 2).

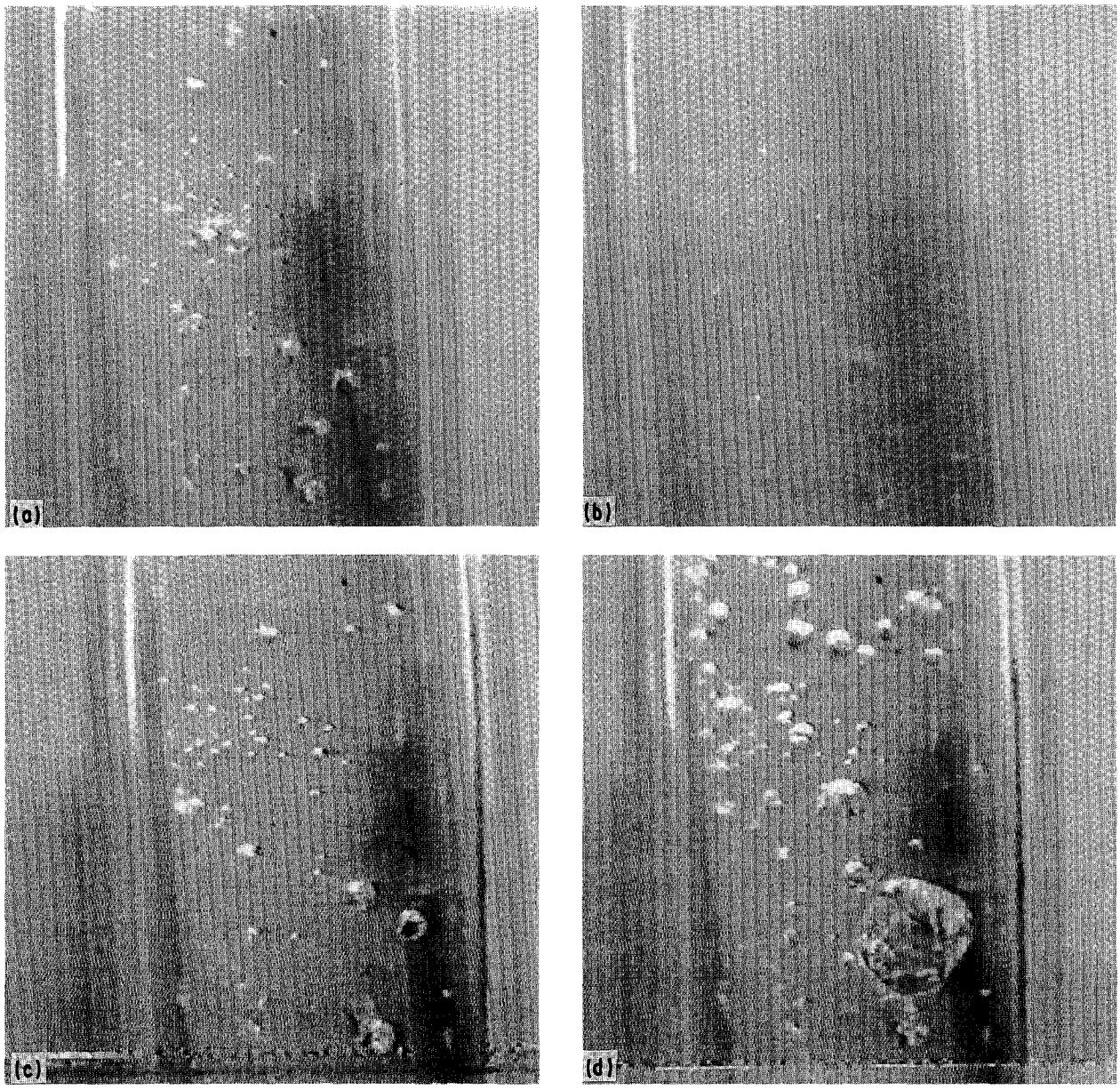

Figure 2 Photographs of the pure PDMS sample with internal bubbles as microcracks initiate due to internal gas pressure. (a) Original sample, atmospheric pressure; (b) sample at 3 MPa, just after pressure has been applied; (c) cracks around the bubbles, after a few minutes at 3 MPa internal pressure; (d) cracks at their final extension, after several minutes.

The micro-cracks initiated and grew extremely rapidly, as in a glassy brittle polymer: their initiation and growth often took place within one single video frame time (1/50 s). Subsequent slow growth also existed. This experiment demonstrated undoubtedly that quasi-fragile microrupture can be induced in PDMS under high negative hydrostatic pressure.

3. Salt flow measurements

As the salt flow did not seem to be controlled by a diffusional mechanism, release experiments were performed with different rubbers and salts to estimate the relevant salt flow mechanism. One set of experiments, at 20 °C, were representative of real cases, using rubber–salt compounds for drug release. These experiments being very time consuming (over 1 year), another set of experiments were performed at 70 °C, in order to follow the whole flow mechanism within a few days. Many similar experiments were performed earlier as reported in the literature [11–20], but, in order to verify numerically the newly proposed quantitative models, detailed measurements were needed.

3.1. Materials

For experiments conducted at 20 °C, two rubbers (Rhône Poulenc PDMS, PDMS-1 and PDMS-2) and two salts (NaI and KIO_3) were tested with three salt granulometries (< 50 μm, 100–200 μm, and 200–400 μm). All samples contained 20 wt% salt, and were moulded to a cylindrical shape of 23 mm diameter and 50 mm length.

For experiments conducted at 70 °C, only the PDMS-1 rubber and iodine salt NaI were used. Care was taken to avoid salt sedimentation during cross-linking of the salt–rubber compound. The salt was kept dry before use. The PDMS monomer and salt mixture was heated under vacuum while being shocked in order to start the curing process. When the

viscosity reached the critical value at which sedimentation is avoided, the compound was poured into cylindrical moulds. The proper temperature cycle was then applied to obtain final curing of the PDMS.

3.2. Realistic case at 20 °C

Each cylindrical sample was introduced into a large water bath. The salt concentration of the bath was continuously measured, and therefore release–time plots could be drawn for each sample (Fig. 3). No observation on the sample itself has been made, except swelling.

These plots lead to the following observations:

(a) The nature of the salt is a major parameter in both PDMS.

(b) Granulometry is more important in PDMS-1 than in PDMS-2.

(c) Coarser granulometry leads to faster salt release.

The release "step" in PDMS-2 at the instant of immersion ($t = 0$) was due to instantaneous dissolution of the salt lying at the surface of the cylinder, and hence proportional to the granulometry. In PDMS-1 this effect did not exist, as during curing, PDMS-1 tends to create a thin pure rubbery layer at the sample surface, preventing any salt grain from being in direct contact with the surrounding water.

The relevant experimental parameters (slope of salt lost) $(1/Q_0)\delta Q/\delta t$ in % per day and the swelling M/M_0 in % after 61 days, are summarized in Table I, where Q is the salt volumes, Q_0 the initial salt content, S the sample weight, S_0 the initial sample weight.

Comparison of the KIO_3 data with those of NaI, leads to the following conclusions.

1. Swelling is always much lower with KIO_3 than with NaI.
2. Salt flow is equal to or faster with KIO_3 than with NaI.
3. For KIO_3, swelling is rubber-nature and grain-size independent.

A comparison of the data obtained for PDMS-1 with those for PDMS-2 leads to the following conclusions.

1. PDMS-2 swelling is equal to or larger than that of PDMS-1.
2. Salt flow in PDMS-1 is equal to or faster than in PDMS-2.

Chemical stability of PDMS-1 and PDMS-2 against NaI and KIO_3 was tested, and could not account for the reported results. The latter are consistent with the following facts.

(a) A large cavity (coarse grain), subjected to the same osmotic pressure as a small cavity (small grain), develops larger tangential stresses at the cavity surface. Therefore, coarse salt granulometry leads to earlier cracking accompanied by less swelling and faster salt flow than small salt granulometry.

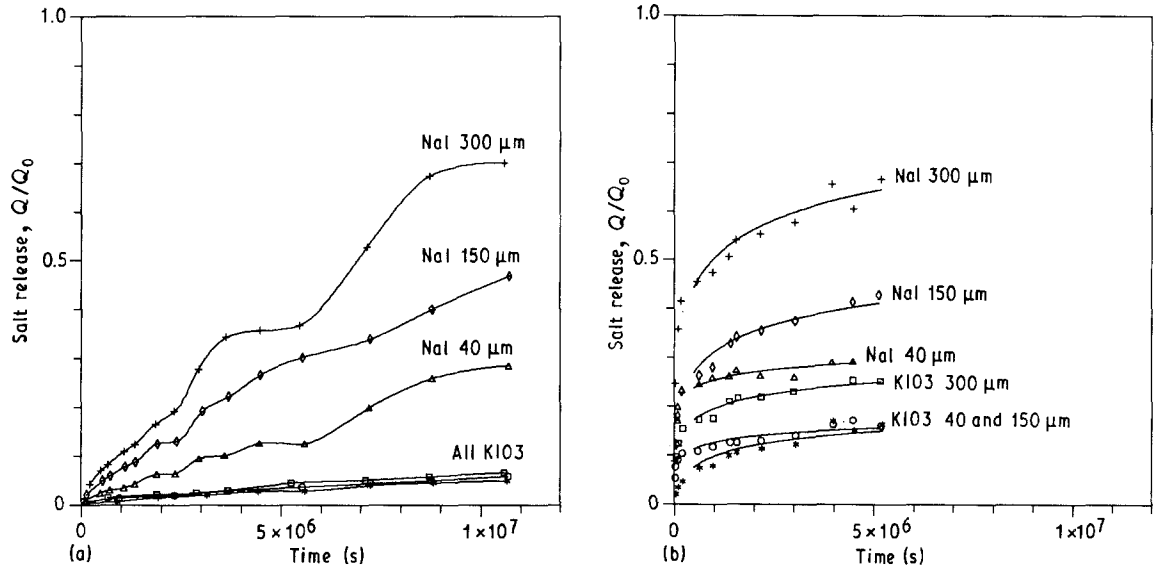

Figure 3 (a) PDMS-1 with NaI and KIO_3. (b) PDMS-2 with NaI and KIO_3. The plots show the relative salt amount lost by the sample as a function of time.

TABLE I

Grain size (µm)	NaI				KIO_3			
	$(1/Q_0)\delta Q/\delta t$ (%/day)		M/M_0 (wt %)		$(1/Q_0)\delta Q/\delta t$ (%/day)		M/M_0 (wt %)	
	PDMS1	PDMS2	PDMS1	PDMS2	PDMS1	PDMS2	PDMS1	PDMS2
< 50	0.21	0.054	13	39	0.049	0.056	2	2.1
100–200	0.41	0.065	11	25	0.049	0.038	2	3
200–400	0.61	0.11	8	13	0.049	0.032	2	3

(b) Osmotic pressure of NaI is about 25 times higher than that of KIO_3. As a result, swelling is much higher with NaI than with KIO_3.

(c) PDMS-2 may undergo much larger strains than PDMS-1 before breakage. The NaI salt flow is faster with less swelling in PDMS-1 than in PDMS-2, because PDMS-1 breaks earlier than PDMS-2.

(d) For very low strains and stresses, which is the case with KIO_3, PDMS-1 and PDMS-2 behave in the same way, namely there are only very few cracks or no cracks at all, and therefore, extremely slow salt flow. The stresses and strains are probably below the critical values for rupture, and only some spurious chemical action leads to a little stress cracking in the rubber, which explains the independence of salt flow against all experimental parameters.

At initial assumption, there were two important independent rubber parameters governing the salt flow: the rupture strain and the rupture stress of the rubber.

3.3. Laboratory case at 70 °C

As mentioned before, two mechanisms controlled the salt flow, namely microcrack front kinetics (referring to rupture properties of PDMS), which in turn was controlled by the osmotic pressure front (referring to water diffusion front kinetics in PDMS). Depending on which of these two mechanisms is the faster rupture properties or water diffusion properties are the limiting factor for salt flow. To evaluate these mechanisms, experiments at 70 °C have been done as follows.

Salt–PDMS cylinders, as previously described, were introduced into a water bath at 70 °C. Both flat ends of the cylinders were sealed to confine water diffusion to the cylindrical surface, ensuring a cylindrical symmetry of the mechanism. At constant time intervals, a 2–3 mm slice was cut from one end of the cylinders in order to examine the inner structure of the cylinder, and the position of the microcrack front and of the water front. The amount of salt lost by the sample to the surrounding water was simultaneously measured.

Fig. 4 shows a schematic drawing of the inner structure of the cylinders. The central region was dry and white, like the original salt–PDMS compound. The outer region was absolutely transparent, suggesting a total dissolution of the salt by water and cracks filled with water. The transient region was a gradient region in which the salt was partially dissolved in water. The position of the microcrack front could not be optically localized, but was definitely located within the outer region. The thickness of the gradient region was temperature dependent: at 20 °C, this region had almost vanished.

Fig. 5 shows the plots of the volumes of the inner dry region, of the outer transparent region, compared with the salt lost by the sample. These plots were normalized to facilitate comparison. Several important observations resulted.

(a) The decrease in volume of the inner dry region was grain-size independent. The volume variation of this region depended on the velocity of the water front propagating into the salt–PDMS compound. As shown later, this independence was consistent with a simple model.

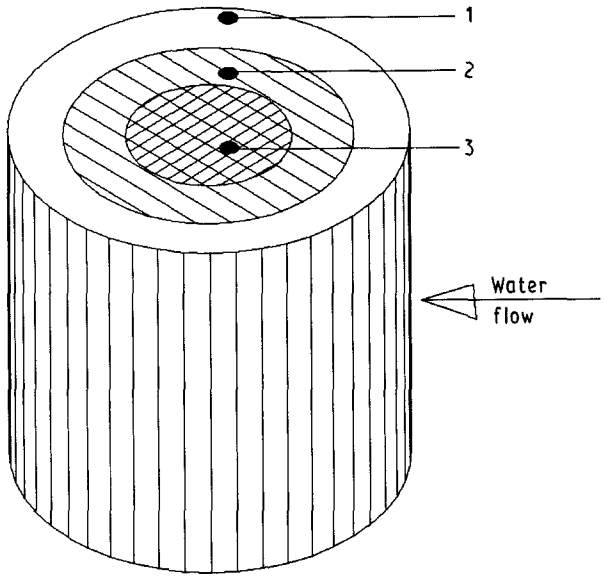

Figure 4 The inner structure of the salt–PDMS cylinders during release: there were three regions, from surface to core: 1, the fully "wet" region; 2, the gradient region; 3, the fully "dry" core region. The microcrack front lies within the external region 1. The internal stresses are due to swelling: the "dry" core was rigid and incompressible, the outer region was dilated by the water absorption and the wet salt osmotic pressure, the global geometry was enforced by the rigid core. Therefore, the core was under tangential tension and hydrostatic negative pressure, the outer region under tangential compression and hydrostatic positive pressure, and the transient region under tangential stresses varying from positive to negative.

(b) The lost salt volume was always lower than the volume of the outer transparent region. As the salt could be lost only through the cracks, the microcrack front must have been within the transparent region.

(c) It may have been possible that the crack front was the boundary of the transparent region or, in other words, that the salt lost was equal to the volume of that region. Considering the stresses in the sample in Fig. 4, the external region (from where the salt was lost) was under compression as long as the rigid core maintained the sample geometry: the microcracks were reclosed by the compression, and salt flow was slowed down. Once the rigid core vanished, this compression vanished too, and salt flow sped up and the lost salt volume tended to the volume of the external region, as shown in Fig. 5, especially for the 200–400 μm grain size. The trend corresponded well to the curvatures of salt loss plots. Fig. 6 shows that the salt lost with time at 20 and 70 °C exhibited the same trends due to internal stresses.

3.4. Water front in the compound

The kinetics and rate effects of the propagation of the water front are difficult to elucidate. As mentioned in the literature, temperature increases the rate of the process [3], and due to the large amount of water needed to dissolve the salt pockets, the saturation equilibration process is orders of magnitude slower than that in pure PDMS [10], with a sharp water front. However, a very crude estimation of the propagation was done in the following manner.

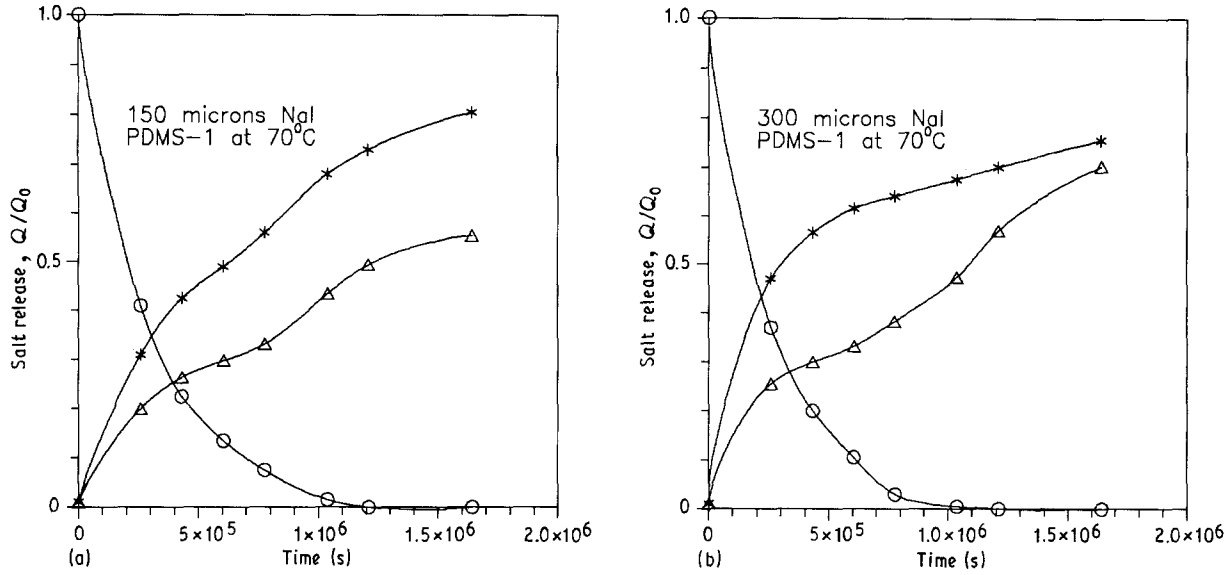

Figure 5 Normalized volumes of the inner dry core, of the outer transparent region and of the salt lost by the sample. (a) PDMS-1 with 20 wt % salt, grain size 100–200 μm; (b) as (a) but for grain size 200–400 μm; 70 °C. (*) External transport volume, (○) internal core–volume, (△) released salt volume.

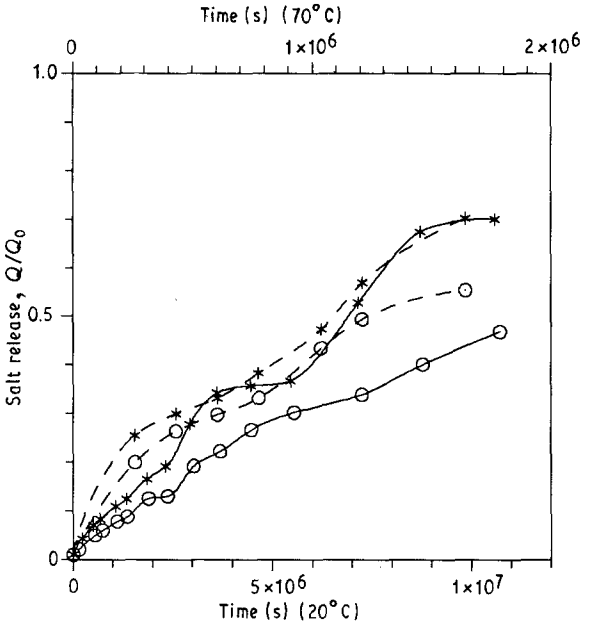

Figure 6 Comparison of salt volume lost by the sample at (——) 20 and (– – –) 70 °C for two grain sizes: (*) 300 μm, (○) 150 μm. Note the fact that the curves are the same, with only a time-scale change.

As the saturated water content of salt is about 100–1000 times the content of saturated PDMS, each salt grain acts as a "trap" for the water. Assuming the water flow through PDMS between salt grains to remain constant, the time to fill up a salt grain is two to three orders of magnitude higher than that to fill up the same volume of PDMS. Hence retardation of the equilibrium may have been of the order of magnitude of the salt volume fraction in the compound, times the ratio between the saturated water content of salt and PDMS. Such an effect does not primarily depend on grain size, but on salt volume fraction of the compound. No rupture phenomena were supposed to have occurred. This actually occurs before or after the salt grain is entirely dissolved, as will be shown later.

4. Fracture measurements of the silicone rubber

As the salt exchange takes place by means of the microcrack network, it is of primary importance to investigate some relevant fracture property of the rubber. Unfortunately, rubber can be subjected to large deformations prior to fracture, making it very difficult to define such a fracture criterion. Intrinsic fracture properties (independent of sample geometry) are properly defined only in brittle materials, exhibiting extremely low deformations prior to fracture. Fortunately, in the case of osmotic pressure fracture, the stress inducing the cracks around the holes is a simple hydrostatic pressure. Therefore, one can expect that a fracture test using a pre-cracked sample with a geometry leading to a hydrostatic negative pressure at the crack tip might yield crack initiation and growth criteria relevant for osmotic pressure failure. It is known that crack tips are subjected to high negative hydrostatic pressure (the case of crazing in glassy polymers) when a fully plane strain situation exists. This is obtained by using very thick pre-cracked samples, where the thickness is large compared to crack tip radius. On the other hand, the overall deformation of the sample, far from the crack tip must remain small to ensure valid fracture mechanics. Owing to the low tensile modulus of the silicone rubber, this requirement was difficult to achieve. As a result, a strip specimen as shown in Fig. 7 was chosen [20]. The fracture toughness in this specimen is defined for rigid materials (Fig. 7).

Measurements on PDMS (which is not a rigid material) showed that "brittle" crack propagation occurs in PDMS with an overall strain less than 10% at the boundary, with crack-tip radii less then 0.1 mm. In fact, for rubbery materials, the fracture toughness yields [21]

$$G_{1c} = h_0 W_c \quad (1)$$

where W_c is the stored elastic energy density per unit

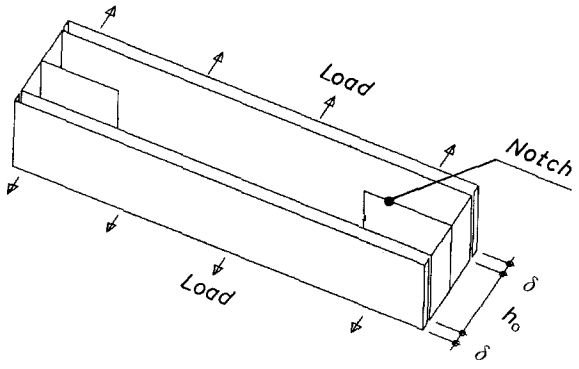

Figure 7 Strip fracture test specimen. The specimen is loaded along its length. If the displacement is kept constant during crack growth, the energy release rate remains constant. Consequently, the crack speed can be easily controlled over several decades, and intrinsic fracture toughness, G_{1C}, measured as $G_{1C} = E\Delta D h^2 (2h_0)^{-1}$, where E is the tensile modulus of the material, h_0 the initial height, and Δh the grips displacement. Sample thickness is 25 mm, length 250 mm and height 20 mm.

volume. For a linear elastic rubber with constant tensile modulus, E, like PDMS,

$$W_c = E\,\Delta h^2/2h_0^2 \quad (2)$$

and hence

$$G_{1c} = E\,\Delta h^2/2h_0 \quad (3)$$

as defined for brittle materials. As a consequence, G_{1c} or K_{1c} can be used in all calculations, with the relation

$$G_{1c} = K_{1c}^2/E \quad (4)$$

Although the tensile modulus of PDMS was not perfectly constant, measured values for G_{1c} versus crack speed seem to be consistent. To avoid unexpected spurious bending, the sample was fully symmetrical with two razor blade notches, one at each end. Regularly spaced lines were marked on the lateral face, allowing the recording of the crack speed. Special grips were built to hold the specimens. Each specimen was slowly loaded up to a certain mean displacement, Δh. Owing to imperfection in the symmetry, only one of the notches started to grow. The growth was followed over a few millimetres to measure the velocity. The load was removed, and the other notch was enlarged with the razor blade to obtain once again a fully symmetrical specimen. Then another measurement could be performed on the same sample.

It had been verified that the measured fracture toughness is crack-length independent. Hence, as an initial approximation, the measured toughness could be considered as an intrinsic fracture property, despite the unusually low mechanical properties. The notches propagated smoothly, following a planar trajectory without side grooves on the specimen. The fracture surface of pure PDMS was visually perfectly flat and smooth, like a mirror, as observed in brittle glassy polymers.

Two types of measurements were performed: fracture toughness, $G_1(\mathring{a})$, for pure PDMS rubber, where $\mathring{a}$ is the crack speed and fracture toughness, $G_1(100\ \mu m\,s^{-1})$, for an iodine salt–PDMS compound.

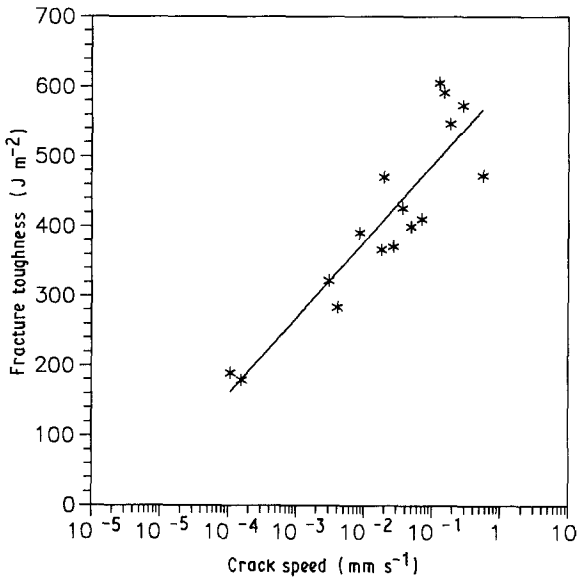

Figure 8 The fracture toughness versus crack speed in pure PDMS. The data appeared to follow a straight line drawn on a semi-log plot. Extremely low speeds were technically difficult to achieve. Therefore, the line was extrapolated over one or two decades to estimate toughnesses at lower speeds. The toughness was about 1/30 of that of a glassy polymer (1 MPam$^{1/2}$).

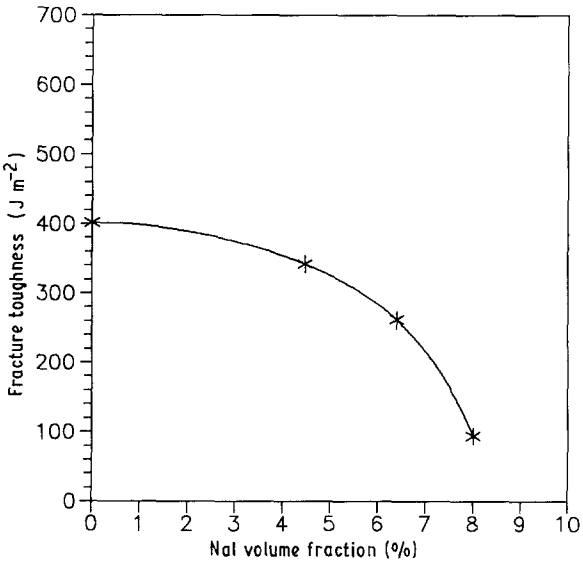

Figure 9 Fracture toughness of the PDMS–salt compound at 0.1 mm s^{-1} as a function of iodine salt content. The fracture toughness would probably not decrease towards zero at higher salt contents, as the plot might suggest. The decrease in toughness with salt content is probably simply due to the weak adhesion between salt and PDMS.

5. Fracture toughness versus osmotic pressure

Assuming that the fracture properties of PDMS are known, the onset of microcracks around a swollen salt pocket may be calculated in two steps: first, the equilibrium pressure of the swollen pocket must be calculated, and then compared with its strength.

5.1. Osmotic pressure of the salt in the PDMS

For an ideal salt solution, the osmotic pressure is classically expressed as [3]

$$\pi = nRT v_2^{-1} S_2 (1 - S_2)^{-1} \quad (5)$$

where T is the temperature (K), $R = 0.082055$ $dm^3\ 10^5\ Pa\ K^{-1}\ mol^{-1}$, v_2 is the molar volume, S_2 is the volume fraction of solute in solution, and n the moles of particles formed upon solution of 1 mol solute ($n = 2$ for NaI). For a saturated solution of NaI, the solute fraction is about 65 wt% at 20 °C and 70 wt% at 70 °C. Then it was a simple matter to estimate that the order of magnitude of the osmotic pressure may reach up to 30 MPa.

On the other hand, the rubber around an isolated salt pocket of radius $r_0 = \langle D_0/2 \rangle$, when inflated to a radius $r = \langle D/2 \rangle$, applies a pressure [3]

$$P = (5 - 4\lambda^{-1} - \lambda^{-4})G/2 \quad (6)$$

where G is the shear modulus of the rubber (1.1 MPa for PDMS)

$$\lambda = r/r_0 = \langle D \rangle / \langle D_0 \rangle \quad (7)$$

Hence, the highest pressure applied by the rubber, when r becomes infinite, is equal to $5G/2$, which is about 3 MPa for PDMS and one order of magnitude lower than the maximum osmotic pressure. Consequently, water will enter the salt pocket until full dissolution of the salt occurs, and even further, until the salt solution is diluted enough to reach the equilibrium

$$P = \pi \quad (8)$$

For NaI, the numerical values show that the pressure equilibrium was reached at $S_2 = 1.2\%$, $\pi = 2.2$ MPa, $\lambda = 4.4$. It is noteworthy that G and π both increase linearly with T, (for thermodynamical reasons) and the values of S_2 and λ do not depend on the temperature and size of salt pockets [3].

When the pressures were equal, equilibrium was reached between the salt, the PDMS and the absorbed water. It was implicitly assumed that the rubber does not break under these conditions.

5.2. Rupture of a spherical hole in rubber

Once an intrinsic valid fracture criterion for pure PDMS and values of osmotic pressures have been obtained, the rupture of the swollen salt pocket must be studied. If one assumes that the salt water has only little effect on the mechanical properties of PDMS and that the swollen salt pockets are spherical, the Williams and Schapery [22] analysis can be used. They established a classical energy balance for a hole in an infinite elastic medium subjected to hydrostatic pressure. The medium is supposed to be perfectly elastic with Neo-Hookean behaviour. The analysis yields a critical value for the hole internal pressure, P_c, and for the extension ratio, λ_c. The critical values are a function of the hole diameter, $\langle D_0 \rangle$, the tensile modulus, E, of the medium, and the fracture surface energy, G_{1c} or K_{1c}

$$\lambda_c^6 - (k + 3/2)\lambda_c^4 + 1/2 = 0 \quad (9)$$

and

$$P_c = (5 - 4\lambda_c^{-1} - \lambda_c^{-4})E/6 \quad (10)$$

where $k = 6K_{1c}^2 E^{-2} \langle D_0/2 \rangle^{-1} = 6G_{1c} E^{-1} \langle D_0/2 \rangle^{-1}$.

Fig. 10 shows the values for P_c and λ_c as a function of the reduced material parameter, k. G_{1c} or K_{1c} are threshold values of $G_1(\mathring{a})$ or $K_1(\mathring{a})$ for $\mathring{a} = 0$ (zero crack speed). The actual salt pockets are obviously not perfectly spherical, as salt grains have irregular shapes. Nevertheless, micrographs have shown that, when dissolved and swollen, the pockets tend towards spherical shape. On the other hand, the assumption of isolated pockets is valid only up to salt volume fractions of a few per cent in the compound.

Experimental measurements of E, $K_{1c}(\mathring{a})$ for PDMS and $\langle D_0 \rangle$ at 20 °C gave the results shown in Table II (the critical threshold value, K_{1c}, was estimated to be the value of K_1 at about 10^{-5} mm s^{-1}).

The calculated values were rather rough, as neither grain size, $\langle D_0 \rangle$, nor front speed had been well defined. Nevertheless, K_{1c} at 10^{-5} mm s^{-1} was an overestimated value for the threshold K_{1c}, and hence, k, pressure, P_c, and extension, λ_c, were overestimated as

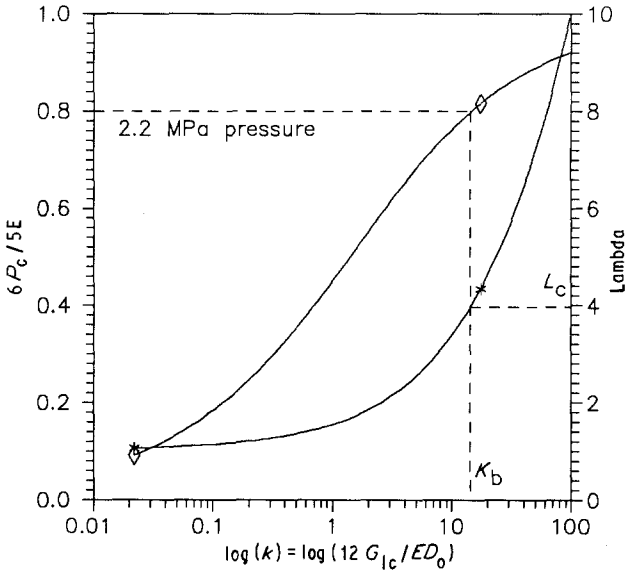

Figure 10 (*) Critical extension, λ_c, and (◇) critical internal pressure, P_c, $(6P_c/5E)$ at instability for a spherical cavity in an infinite elastic Neo-Hookean medium as a function of the reduced material parameter: $k = 6K_{1c}^2 E^{-2} \langle D_0/2 \rangle^{-1} = 6G_{1c} E^{-1} \langle D_0/2 \rangle^{-1}$.

TABLE II

Grain size (μm)	K_{1c} ($Pam^{1/2}$)	k	Breakage		Equilibrium	
			λ_c	P_c (MPa)	λ_e	P_e (MPa)
300	15000	1.45	1.7	1.4	4.4	2.2
150	15000	2.9	2.2	1.7	4.4	2.2
40	15000	11	3.6	2.1	4.4	2.2

well. So, λ_c and P_c were lower than those at equilibrium. Hence, cracks arose around the salt grains before equilibrium was reached, but not necessarily before full dissolution of the salt in the pocket.

5.3. The microcracking regimes

The initial volume of the cavity, v_0, is that of the dry salt, and the volume, v_t, at any further moment is equal to $\lambda^3 v_0$. Hence the amount of water in the pocket is equal to $v_0(\lambda^3 - 1)$, and the volume fraction, S_2, is given by

$$S_2 = \lambda^{-3} \tag{11}$$

Fig. 11 shows the major parameters P_c, λ_c and S_2 plotted on the same graph. The graph also shows the two limits for the reduced variable, k. These limits represent:

(i) k_A, the value of k corresponding to the upper limit S_2^* below which the salt grain is fully dissolved (for NaI, about 20%). If k is above that value, cracking occurs when salt is fully dissolved in the pocket;

(ii) k_B, the value of k corresponding to the equilibrium pressure and extension of the salt pocket. If the value of k is above that limit, no cracking occurs, the equilibrium pressure is lower than the cracking pressure.

Depending on the relative positions of limits k_A and k_B, many cases are possible. Nevertheless, for highly soluble salts, k_A is generally lower than k_B (with reference to the values of λ), and the rubber–salt compounds behave in the following way, as a function of k.

(a) If k is below k_A, cracking occurs before the salt is dissolved in pockets. This seemed to correspond to the 70 °C experiments reported here. The white gradient zone corresponds to the zone where cracks existed, with still undissolved salt in the pockets, and hence, opaque compound.

(b) If k is between k_A and k_B, cracking occurs when salt grains are fully dissolved, but not at equilibrium. Then the compound is transparent before cracking. This situation corresponded to the 20 °C experiments reported here with the finest grain size. There was always a water gradient ahead of the moving front behind which the salt pockets were fully dissolved. It is known that, due to the high water content of the salt pockets with regard to the water content of the PDMS (three orders of magnitude), the moving front was very sharp and the gradient zone very small.

(c) If k is above k_B, salt pockets reach an equilibrium without cracking. This corresponded to the situation reported here with PDMS-2 rubber (low tensile modulus, E, high fracture toughness, G), and/or very small grain sizes: there is no cracking, and hence, almost no salt flow.

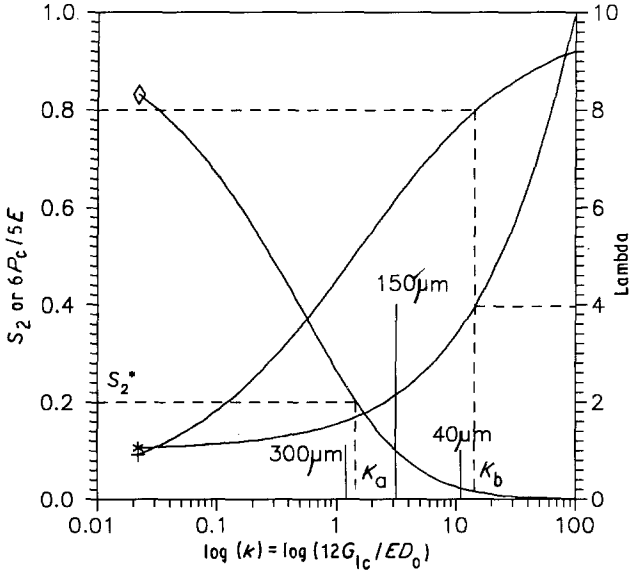

Figure 11 The plot shows (*) critical extension ratio, λ_c, (+) critical pressure, $P_c(6P_c/5E)$, and (◇) salt volume fraction, S_2, in the salt pockets. The particular limits for equilibrium pressure and extension are shown for the case of PDMS and NaI, and the particular value of S_2^* for NaI is also plotted. Three regimes of cracking are possible, as a function of the value of k, below k_A between k_A and k_B, and above k_B.

5.4. Salt release rate

The final step of the calculation was an estimation of the salt release rate $(1/Q_0)\delta Q/\delta t$ as a function of the rupture properties of the PDMS. The following assumptions were made.

(a) The most time-consuming process is the swelling of the salt pockets by the addition of water (of the order of days in real experiments).

(b) The fracture, once the pocket reaches an instability pressure is quasi-instantaneous. The mean distance between two grains is of the order of magnitude of the grain size, and the fracture propagation time to the next grain is negligible.

(c) The duration of the liquid exchange driven through the micropipes by osmotic pressure of the pocket suddenly broken is also negligible compared to the swelling durations.

The calculation consisted of evaluating the time to swell the salt pockets to the critical pressure, in other words, the time it takes for the front to move the mean distance between grain centres.

The PDMS–salt compound was geometrically defined by the following factors: φ, salt volume fraction in the compound; $\langle D_0 \rangle$, mean salt grain diameter; $\langle A \rangle$, mean grain centre to centre distance; $\langle B \rangle$, mean grain border to border distance; Φ, water flow in PDMS per unit time and unit area at the PDMS–salt interface. For simple geometrical reasons

$$\langle A \rangle = \langle D_0 \rangle \varphi^{-1/3} \tag{12}$$

and

$$\langle B \rangle = \langle D_0 \rangle (\varphi^{-1/3} - 1) \tag{13}$$

It was assumed that PDMS permeability was hardly influenced by the salt, and that the water activity in a salt pocket remained almost constant until all the salt was dissolved in the pocket [10]. Given that Φ was the water flux per unit time and surface at the pocket interface (Φ is constant for a given compound), the equations for the grain size and salt volume fraction effects could be derived.

5.4.1. Grain-size effect

The initial salt grain has a volume of $\langle D_0 \rangle^3$ while the swollen pocket has a volume of $\lambda^3 \langle D_0 \rangle^3$ and a surface of $\lambda^2 \langle D_0 \rangle^2$. The water content of the swollen pocket is $(\lambda_c^3 - 1)\langle D_0 \rangle^3$. The water flow at the pocket surface is equal to $\Phi\lambda^2 \langle D_0 \rangle^2$ at any moment during swelling. The integration of that equation over the swelling duration shows that the critical time it takes to swell the grain is

$$\tau_c = 3\langle D_0 \rangle(\lambda_c - 1)/\Phi \quad (14)$$

The crack jumps to the next grain over a distance defined earlier as $\langle A \rangle$, and the mean velocity is

$$\langle v_c \rangle = \Phi\varphi^{-1/3}/\{3(\lambda_c - 1)\} \quad (15)$$

This velocity depends on grain size via λ, and hence on the reduced variable, k. It is straightforward that the steady state salt release flow per unit time and surface is equal to $\varphi \langle v_c \rangle$

$$\delta^2 Q/\delta t \delta S = \Phi\varphi^{2/3}/[3(\lambda_c - 1)] \quad (16)$$

If Q_0 is the initial salt volume of the compound item of surface, S_0, and volume, V_0, then the normalized integral flow is

$$(1/Q_0)\delta Q/\delta t = (S_0/V_0)\Phi\varphi^{-1/3}/[3(\lambda_c - 1)] \quad (17)$$

As Φ may depend on φ, Equation 15 can be tested only by varying λ, and the equation is simplified to obtain the salt release

$$(1/Q_0)\delta Q/\delta t = \alpha(\lambda_c - 1)^{-1} \quad (18)$$

The coefficient, α, includes physical parameters of the compound and the water diffusion property of the PDMS. The reduced salt release has been plotted in Fig. 12, as a function of k.

Fig. 12 shows that the limiting value, k_B, for k, above which equilibrium was reached before rupture, prohibited release rates lower than $\simeq 0.3\alpha$. With the experimental values reported here, the smallest threshold value for $(1/Q_0)\delta Q/\delta t$ was $\simeq 1.7 \times 10^{-8}\ s^{-1}$, using a grain size of about 30 μm. The experimental values are summarized in Table III. As

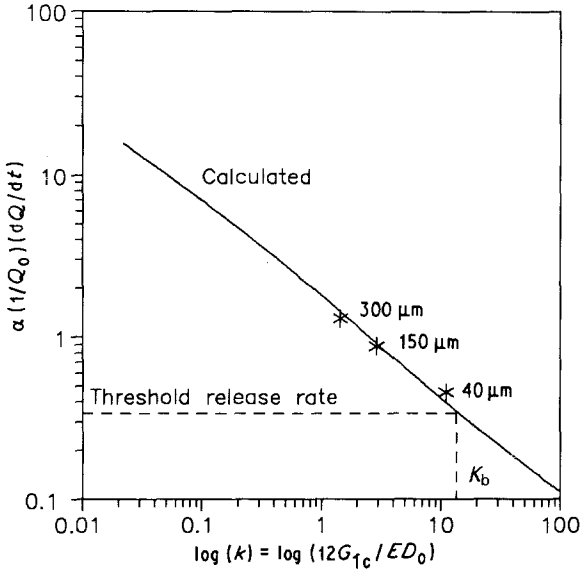

Figure 12 The reduced calculated salt release rate $(1/\alpha)\ (1/Q_0)\delta Q/\delta t$ as a function of the fracture toughness, G, the tensile modulus, E, of the PDMS and the grain size, $\langle D_0 \rangle$. Experimental values are also reported.

α is almost constant for all experiments, the model describing the influence of the grain size was probably correct.

5.4.2. Salt volume fraction effect

The scaling law of the influence of φ upon Φ is not straightforward. Simply assume that the water flow Φ per unit time and surface at the pockets surface is proportional to the amount of water trapped in the compound near the considered pocket. This amount being essentially trapped in the salt grains (hence in the volume fraction φ of the compound), Φ was estimated proportional to φ. Then, the salt release becomes:

$$(1/Q_0)\delta Q/\delta t = \beta(S_0/V_0)\varphi^{2/3}/[3(\lambda_c - 1)] \quad (19)$$

The experimental results for varying φ are summarized in Table IV. Again, β was almost constant and equalled $0.421 \times 10^{-8}\ m\,s^{-1}$. Then, the release rate

TABLE III

$\langle D_0 \rangle$ (10^{-6} m)	k	φ	S_0/V_0 (m^{-1})	$Q_0^{-1}\delta Q/\delta t$ ($10^{-8}\ s^{-1}$)	$(\lambda_c - 1)^{-1}$	α ($10^{-8}\ s^{-1}$)
40	11	0.08	214	2.46	0.4	6.15
150	2.92	0.08	214	4.75	0.91	5.2
300	1.44	0.08	214	7.02	1.4	5.01

TABLE IV

$\langle D_0 \rangle$ (10^{-6} m)	$k = 12G/E < D_0$	φ	S_0/V_0 (m^{-1})	$Q_0^{-1}\delta Q/\delta t$ ($10^{-8}\ s^{-1}$)	$1/3(\lambda_c - 1)$	$\beta(10^{-8}\ ms^{-1})$
150	2.91	0.056	214	4.06	0.303	0.429
150	2.91	0.064	214	4.49	0.303	0.418
150	2.91	0.072	214	4.69	0.303	0.418
150	2.91	0.080	214	5.17	0.303	0.429
150	2.91	0.100	214	5.51	0.303	0.395

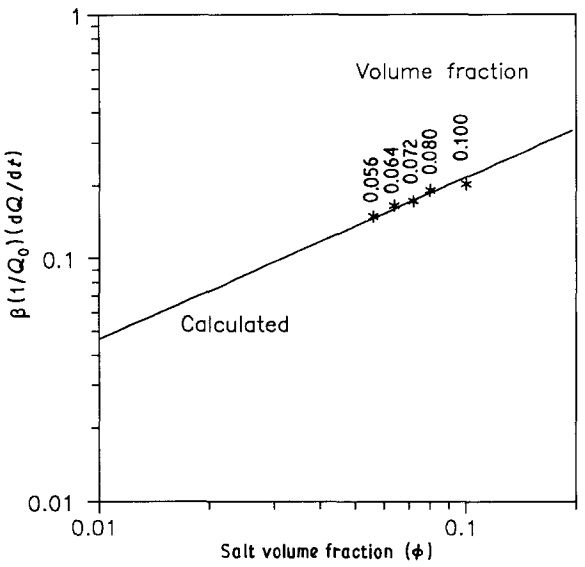

Figure 13 The reduced calculated salt release rate $(1/\beta)\,(1/Q_0)\,\delta Q/\delta t$ as a function of the content, φ, in the PDMS compound. Experimental values are also reported with $\beta = 0.421\ 10^{-8}\ m\,s^{-1}$.

could finally be written as

$$(1/Q_0)\delta Q/\delta t = 0.421 \times 10^{-8}(S_0/V_0)\varphi^{2/3}/[3(\lambda_c - 1)] \quad (20)$$

It should be noted that β included only water-diffusion properties of PDMS, as osmotic salt properties and PDMS rupture properties had been modelled. Fig. 13 shows the release rate as a function of φ.

The geometrical variable, S_0/V_0, has not been tested. As a matter of fact, all experimental values were obtained based on cylindrical samples, whose S_0/V_0 varied greatly during experiments, either due to swelling or to the fact that the "active" part of the compound decreased during the experiment. S/V in an experiment changes from S_0/V_0 to infinite when the "active" volume tends to zero.

6. Conclusions

The salt release rate is controlled by the reduced variables, k. Small values of k lead to fast salt flow, which corresponds to coarse salt grains, $\langle D_0 \rangle$, low fracture toughness, K_{1c} or G_{1c}, or high tensile modulus, E. The compound is characterized by the coefficient β, representing the water diffusion properties in PDMS.

Rubber–salt compounds behave in the following way, as a function of k:

1. If k is below the limit, k_A (low fracture toughness, high tensile modulus, high grain size), cracking occurs before the salt has dissolved in its pockets.

2. If k is between k_A and k_B, cracking occurs when salt grains are fully dissolved. At that level of water absorption, the pockets are almost spherical and the shape of the initially dry salt grains is less important. This situation corresponded to 20 °C experiments reported here, close to the limiting value of k_B.

3. If k is above the limit k_B, salt pockets reach an equilibrium without cracking. This corresponded to the situation reported here with the PDMS-2 rubber (low tensile modulus, high fracture toughness, very small grain sizes). There was no cracking, and as a result, almost no salt flow.

4. The limiting value, k_B, corresponds to a minimum threshold value of salt release, below which release stops.

5. A semi-empirical law for the salt release rate as a function of rubber toughness and tensile modulus, and as a function of osmotic pressure, granulometry and volume fraction of the salt has been derived.

6. The swelling of the rubber compound was partially controlled by its geometry through the dry undeformable core. This swelling parameter is, therefore, experimentally not really relevant; despite this it has been largely used to explain many results in the literature.

References

1. P. J. FLORY, "Principles of Polymer Chemistry" (Cornell University Press, Ithaca, New York, 1953) Ch. XII.
2. G. J. BRIGGS, D. C. EDWARDS and E. B. STOREY, *Rubber Chem. & Techn.* **36** (1963) 621.
3. R. F. FEDORS, *Polymer* **21** (1980) 207.
4. S. GLASSTONE, "Textbook of Physical Chemistry" (Van Nostrand, New York, 1958) p. 671.
5. A. N. GENT and P. B. LINDLEY, *Proc. R. Soc. Lond.* **A249** (1958) 195.
6. D. H. KAELBLE, *Rev. Macromol. Sci.* **C6** (1971) 85.
7. D. E. ROSNER, *J. Phys. Chem.* **73** (1969) 382.
8. R. F. FEDORS, *Polym. Lett. Edn.* **12** (1974) 81.
9. J. A. BARRIE and D. MACHIN, *J. Macromol. Sci. Phys.* **B3** (1969) 673.
10. *Idem., ibid.* **B3** (1969) 645.
11. R. GALE, S. K. CHANDRAZEKARAN, D. SWANSON and J. WRIGHT, *J. Membr. Sci.* **7** (1980) 319.
12. W. E. ROORDA, M. A. DE VRIES, C. KOSHO, L. G. J. DE LEEDE, A. G. DE BOER and H. E. JUNGINGER, in Proceedings of 4th International Conference on Pharmaceutical Technology, Paris 1986, Vol IV, pp. 292–98.
13. V. CARELLI, G. DI COLO, C. GUERRINI and E. NANNIPIERI, *Int. J. Pharmaceut.*, to be published.
14. V. CARELLI, G. DI COLO and E. NANNIPIERI, *Il Farmaco-Ed. Pr.* **43** (1988) 121.
15. V. CAMPILGLI, G. DI COLO, E. NANNIPIERI and M. F. SERAFINI, *ibid.* **43** (1988) 57.
16. V. CARELLI, G. DI COLO and E. NANNIPIERI, *Int. J. Pharamaceut.* **35** (1987) 21.
17. G. DI COLO, V. CARELLI, E. NANNIPIERI, M. F. SERAFINI and D. VITALE, *ibid.* **30** (1986) 1.
18. G. DI COLO, V. CAMPIGLI, V. CARELLI, E. NANNIPIERI, M. F. SERAFINI and D. VITALE, *Il Farmaco-Ed. Pr.* **39** (1984) 310.
19. V. CARELLI and G. DI COLO, *J. Pharamaceut. Sci.* **72**, (1983) 316.
20. PARIS and SIH, in "Fracture Toughness Testing and its Application", STP 381 (1965) 30-81 (ASTM, Philadelphia, PA, 1965). ASTM Special Technical Publication 381 (1965) pp. 30–81
21. A. J. KINLOCH and R. J. YOUNG, in "Fracture Behaviour of Polymers" (Applied Science, London, 1983) pp. 97–106, 370–420.
22. M. L. WILLIAMS and R. A. SCHAPERY, *Int. J. Fract. Mech.* **1** (1964) 64.

Received 14 March
and accepted 1 July 1991